Fifth International Symposium on Marine Propulsors
smp'17, Espoo, Finland, June 2017

RANSE-based Simulation and Analysis of Scale Effects on Open-Water Performance of the PPTC-II Benchmark Propeller

Xiao-Qian Dong, Wei Li, Chen-Jun Yang*, Francis Noblesse

Collaborative Innovation Center for Advanced Ship and Deep-Sea Exploration (CISSE),
State Key Laboratory of Ocean Engineering (SKLOE), Shanghai Jiao Tong University, Shanghai 200240, China

ABSTRACT

This paper presents our numerical study of the scale effects on a tip-rake propeller, the PPTC-II, based on the RANS simulations using software FLUENT 6.3. The low *Re* option in SST *k-ω* model is adopted at model scale, together with fine prism grids to resolve the viscous sub-layer. At full scale, standard wall function is adopted. The scale-effect corrections yielded by our RANS simulations are compared with those obtained from the ITTC method. To explain the CFD results, an analysis of sectional forces is performed. To investigate how the tip rake influences propeller scale effects, the geometry of PPTC-II is modified by removing the tip rake only, and the RANS-predicted scale effects for the modified propeller, PPTC-II-m, are compared with those for the PPTC-II. The study indicates that the scale effect on propeller thrust can be as important as that on the torque; somehow the RANS- and ITTC-based predictions for full-scale efficiency agree quite well; the tip-rake reduces tip loading and tip vortex strength, and brings about large differences in the scale effects as compared with the propeller without tip-rake.

Keywords

Propeller; tip rake; open water; scale effect; RANSE

1 INTRODUCTION

Theoretically, the scale effects on propeller open water performance need to be corrected for when predicting the powering performance of a ship. The empirical formulae in the 1978 ITTC Performance Prediction Method (ITTC 2014) (referred to as the ITTC method hereinafter) have been widely used for the correction. In the ITTC method the amounts of correction to model-scale thrust and torque coefficients depend on the model- and full-scale section drag coefficients at $0.75R$, the chord and pitch ratios at the same radius, and the number of blades, where R denotes propeller tip radius. Apparently, the corrections would be the same for two propellers which differ in the skew and rake only. Special tip geometries, such as the tip endplates and tip-rake, are not accounted for in the ITTC method as well. For more accurate prediction of the full scale performance, it is necessary to know how and to what extent the geometric parameters not considered in the ITTC method would influence the results of scale effect corrections. To elucidate the problem and update the present ITTC method for correcting propeller scale effects when possible, the Propulsion Committees of the 27th and 28th ITTC initiated a computational campaign in each term of service using the PPTC, a conventional highly skewed propeller, and the PPTC-II, an unconventional propeller with the tip-rake, respectively. The two test cases were provided by SVA Potsdam, and the data are available to the public at the company's website.

In fact, viscous flow CFD simulation has been almost the only approach for the research of propeller scale effects since the last century (Stanier 1998). The extensive laminar flow region at the Reynolds number of $2\sim3\times10^5$ is an issue which necessitates the use of very fine prism grid layers to resolve the viscous sub-layer and the low *Re* turbulence model at model scale (Krasilnikov et al 2009, Kawamura et al 2009). It was found that the scale effects on propeller thrust and efficiency are underestimated by the ITTC method when compared with the RANS results, especially for highly skewed propellers (Krasilnikov et al 2009). Alternative extrapolation formulae for propeller open water performance were proposed via analysis of RANS simulation results (Müller et al 2009), where the thrust loading, skew, and the changes in magnitude and direction of section force were taken into account in addition to the geometric parameters considered in the ITTC formulae. The comparison for one test case shows that the CFD-based formulae predicts the increments in thrust and efficiency from model- to full-scale are larger than those predicted by the ITTC method.

Propellers with special tips may present new challenges to the ITTC method for predicting propeller scale effects. It was found through CFD simulations that the scale effects on the Kappel and CLT propellers are larger than those on conventional propellers (Hsin et al 2010). More recently, the RANS approach was employed in selecting optimal endplates of the CLT propeller (Sánchez-Caja et al 2014). Besides, the RANS tool was also utilized in the scale effect researches for ducted propellers (Krasilnikov et al 2007) and the rudder bulb (Oh et al 2010).

This paper presents our numerical study of the scale effects on a tip-rake propeller, the PPTC-II, based on the RANS simulations using software FLUENT 6.3. The low *Re* option in SST *k-ω* model is adopted in model scale,

* Correspondence to: cjyang@sjtu.edu.cn.

together with fine prism grids to resolve the viscous sub-layer. At full scale, standard wall function is adopted. The scale-effect corrections yielded by our RANS simulations are compared with those obtained from the ITTC method. To explain the CFD results, an analysis of sectional forces is performed. To investigate how the tip rake influences propeller scale effects, the geometry of PPTC-II is modified by removing the tip rake only, and the RANS-predicted scale effects for the modified propeller, PPTC-II-m, are compared with those for the PPTC-II.

2 MUMERICAL MODELING APPROACH

2.1 Governing Equations

The flow around the propeller working in open water is simulated by solving the RANS equations together with the SST k-ω model for turbulence closure. The continuity and momentum transport equations for an incompressible fluid are written as

$$\left.\begin{aligned} &\frac{\partial(\rho u_i)}{\partial x_i}=0 \\ &\frac{\partial(\rho u_i)}{\partial t}+\frac{\partial(\rho u_i u_j)}{\partial x_j}=\mu\frac{\partial}{\partial x_j}\left(\frac{\partial u_i}{\partial x_j}+\frac{\partial u_j}{\partial x_i}-\frac{2}{3}\delta_{ij}\frac{\partial u_i}{\partial x_j}\right) \\ &\qquad +\frac{\partial}{\partial x_j}\left(-\rho\overline{u_i' u_j'}\right)-\frac{\partial p}{\partial x_i} \end{aligned}\right\} \quad (1)$$

where u_i and u_j (i,j=1,2,3) are the velocity components, p is the static pressure, μ is the dynamic viscosity of water, δ_{ij} is the Kronecker delta, and $-\rho\overline{u_i' u_j'}$ is the Reynolds stress. The transport equations of the SST k-ω model are written as

$$\left.\begin{aligned} &\frac{\partial}{\partial t}(\rho k)+\frac{\partial}{\partial x_i}(\rho k u_i)=\frac{\partial}{\partial x_j}\left(\Gamma_k\frac{\partial k}{\partial x_j}\right) \\ &\qquad +G_k-Y_k+S_k \\ &\frac{\partial}{\partial t}(\rho\omega)+\frac{\partial}{\partial x_i}(\rho\omega u_i)=\frac{\partial}{\partial x_j}\left(\Gamma_\omega\frac{\partial\omega}{\partial x_j}\right) \\ &\qquad +G_\omega-Y_\omega+S_\omega+D_\omega \end{aligned}\right\} \quad (2)$$

where k is the turbulence kinetic energy, ω is the specific dissipation rate, G_k and G_ω denote the generation of k and ω respectively, Γ_k and Γ_ω denote the effective diffusivity of k and ω respectively, Y_k and Y_ω denote the dissipation of k and ω due to turbulence, D_ω is the cross-diffusion term, Y_k and Y_ω are user-defined source terms.

2.2 Computational Model and Setup

The governing equations are solved numerically by means of FLUENT 6.3, a CFD software package based on the finite volume method. Since flow in open water is assumed to be steady and periodic for all blades in the coordinate system fixed to the propeller, a single blade passage suffices for the simulation. As illustrated in Figure 1, the computational domain is a portion of the cylinder which is coaxial with the propeller shaft. It is bounded by a pair of periodic surfaces which pass through the shaft axis and make an angle of 360/Z degrees, where Z is the number of blades. The inlet and outlet of the domain are 5D upstream and 10D downstream of the propeller, where D is the propeller diameter. The radial size of the domain is 10D. As shown in Figure 2, the periodic boundary surfaces pass through the leading and trailing edges of adjacent blades, hence the back and face of the adjacent blades, instead of the same blade, become boundaries of the domain. By doing so, prism layer grids of high quality can be generated easily on blade surfaces, as shown in Figure 3. Using the SST k-ω model for turbulence closure, the boundary layer flow is resolved down to the viscous sub-layer at model scale, while the wall function is adopted at full scale. The wall distance averaged over blade surfaces, y^+, ranges 0.64~1.12 at model scale, and 32~62 at full scale. All the boundary surfaces are discretized via triangular grids, while the space outside the prism layers is discretized via tetrahedral cells. To reduce numerical uncertainties, blade surface grids are geometrically similar at both scales, only the thicknesses of the prism layers are adjusted. The total number of cells is about 4.38 million at both scales.

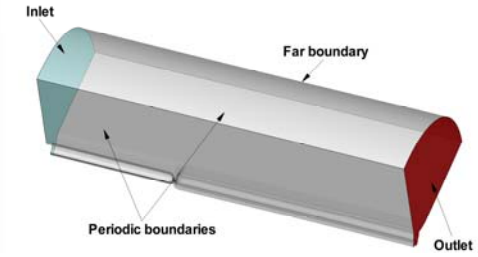

Figure 1 The computational domain

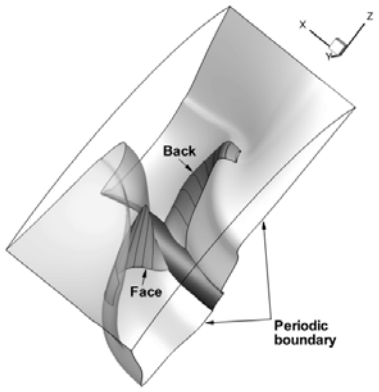

Figure 2 Geometry of the sub-domain enclosing the back and face of adjacent blades

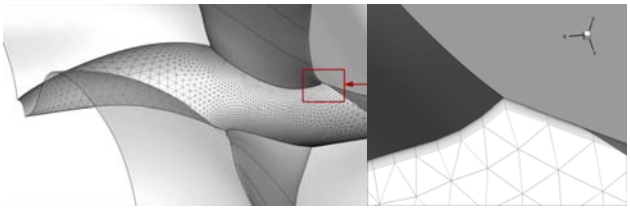

Figure 3 Zoom-up view of blade-surface prism layer grids

The blade, hub, and shaft surfaces are set as stationary no-slip walls in the rotating frame. As shown in Figure 1, the inlet and far boundary are set as velocity inlets, while the outlet as the pressure outlet. For a fixed rotation speed of the propeller, the inlet velocity is specified according to the desired value of J, the advance coefficient.

The convection terms in all the governing equations are discretized with 2nd-order upwind schemes. The SIMPLE scheme is employed for velocity-pressure coupling.

3 RESULTS AND DISCUSSIONS

As shown in Figure 4, the PPTC-II is a four-bladed propeller with a large tip rake. Its geometric data are provided by SVA Potsdam and available in the public domain. The geometric particulars as well as operating conditions of propeller PPTC-II at model- and full-scale are listed in Table 1.

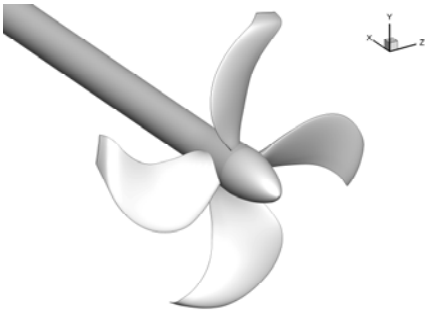

Figure 4 Geometric model of propeller PPTC-II

Table 1 Geometric particulars and operating conditions of propeller PPTC-II at model- and full-scale

	Model-scale	Full-scale
Scale ratio	31.428	1
Number of blades	4	
Diameter [m]	0.23864	7.5m
Chord ratio at 0.75R	0.2331	
Pitch ratio at 0.75R	0.8004	
Rate of revolution (1/s)	18	3.21
Density of water [kg/m^3]	999	1025.87
Kinematic viscosity of water [m^2/s]	1.139×10^{-6}	1.188×10^{-6}
Re at 0.75R, J=0.7	5.571×10^{5}	8.707×10^{7}

3.1 Scale Effects on Open Water Performance

Figure 5 compares the model- and full-scale open water performances of the PPTC-II predicted by CFD, as well as the model-scale EFD data by SVA Potsdam. Except for J=0.1 and J=0.9, the CFD results agree well with EFD data. As is well known, the full-scale efficiency is higher than the model-scale one. However, the increase in full-scale efficiency is largely due to the increase in thrust at J =0.1~0.5; at J=0.7, it is due to the increase in thrust and the decrease in torque, and the latter becomes more important as blade loading decreases.

The ITTC-1978 method is also employed to predict the full-scale performance of PPTC-II by using the RANS results at model-scale. Figures 6 compares the RANS- and ITTC-predicted scale effects on the open water performance. According to the ITTC method, the increase in full-scale efficiency is mainly due to the decrease in torque. On the contrary, the RANS results indicate that, at full scale, the thrust increases by 2~3% (see Figure 6(a)), however, the torque changes little except for J=0.7 (see Figure 6(b)). Amazingly, the increases in full-scale efficiency predicted in both methods differ by less than 0.5% (see Figure 6(c)).

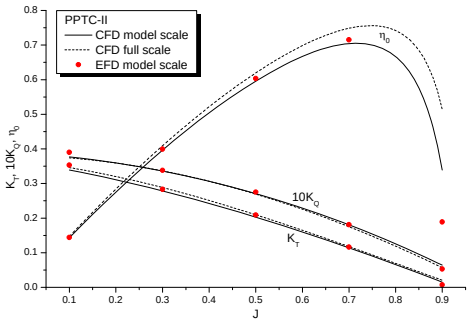

Figure 5 RANSE-predicted open water performances of PPTC-II at model- and full-scale

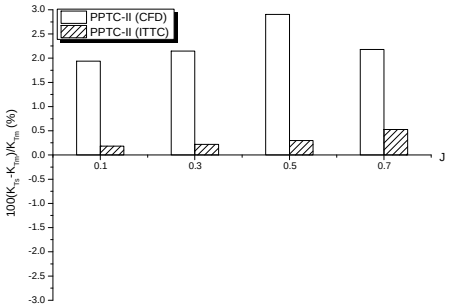

(a) thrust

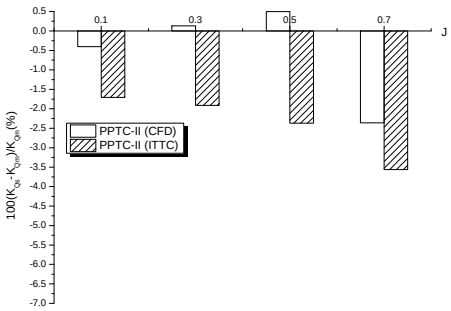

(b) torque

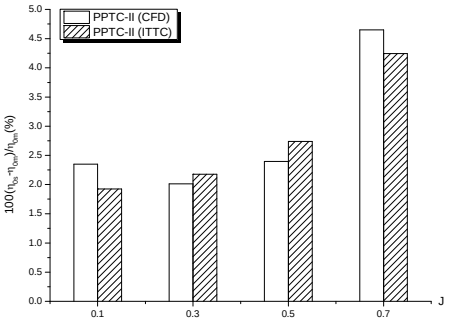

(c) efficiency

Figure 6 Comparison RANS- and ITTC-predicted scale effects on the open water performance of PPTC-II

3.2 Analysis of Sectional Forces

To find out whether the present CFD results can be explained from the physics of flow, and if there are other factors which influence the scale effects in addition to the drag coefficient, an analysis of hydrodynamic forces is conducted on a sectional basis for propeller PPTC-II. The pressure and frictional forces on a blade section are projected onto directions normal and tangential to the nose-tail line and named as section normal and tangential forces respectively. Figures 7 through 9 compare the model- and full-scale normal force coefficients, K_{SN}, K_{SN_P}, and K_{SN_F}, where the subscripts P and F denote pressure and frictional forces respectively. Similarly, the tangential force coefficients are denoted by K_{ST}, K_{ST_P}, and K_{ST_F} respectively, and the results at model- and full-scale are compared in Figures 10 through 12. All the sectional forces are non-dimensionalized by n^2D^3, where n and D are the rate of revolution and the diameter of the propeller respectively, and ρ is the density of water.

As seen in Figure 7, the section normal forces increase at full scale mainly at outer radii over the range of loading conditions investigated. Looking further at Figures 8 and 9, it is obvious that the increase in normal force is primarily due to the pressure component. It is inferred that the section angle of attack becomes larger at full scale due to reduced differences in the displacement thicknesses of boundary layers on the back and face.

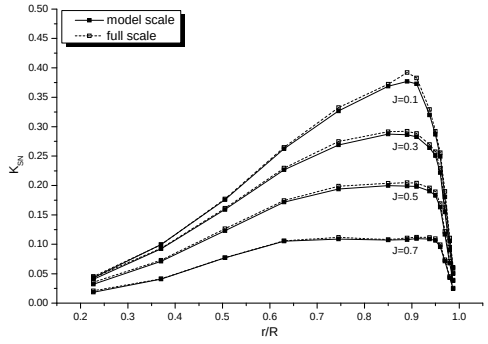

Figure 7 Comparison of section normal forces for PPTC-II

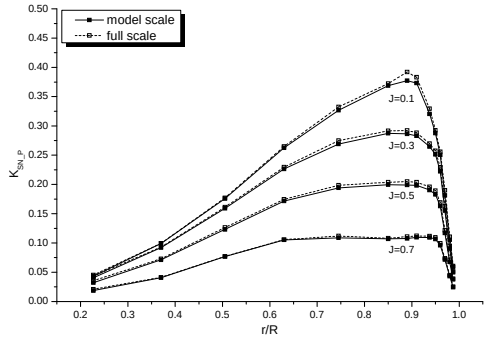

Figure 8 Comparison of the pressure component of section normal forces for PPTC-II

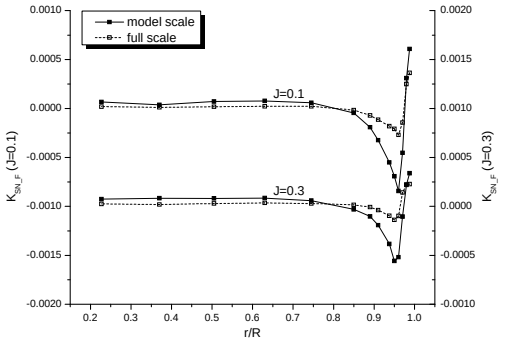

(a)

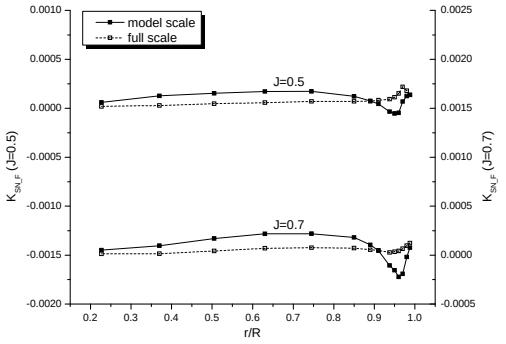

(b)

Figure 9 Comparison of the frictional component of section normal forces for PPTC-II

Figure 10 shows that the section tangential forces decrease at full scale from root to tip over the range of loading conditions investigated. It is clear from Figures 11 and 12 that this result is almost solely due to the decrease in the frictional force.

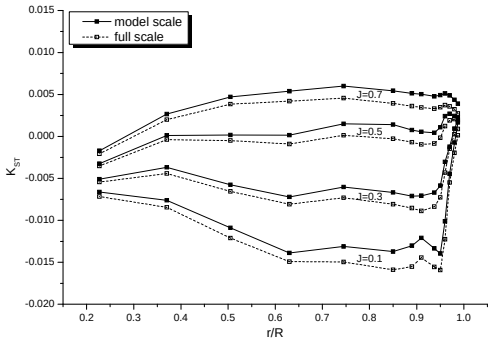

Figure 10 Comparison of section tangential forces for PPTC-II

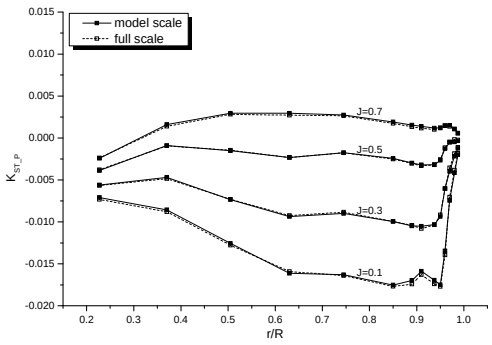

Figure 11 Comparison of the pressure component of section tangential forces for PPTC-II

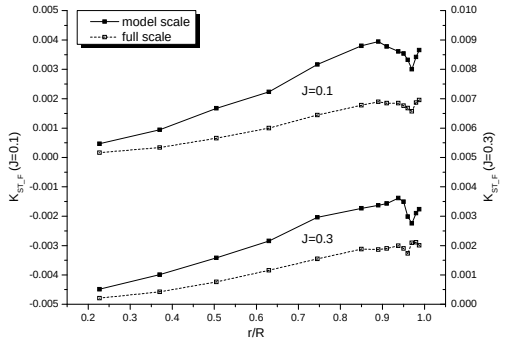

(a)

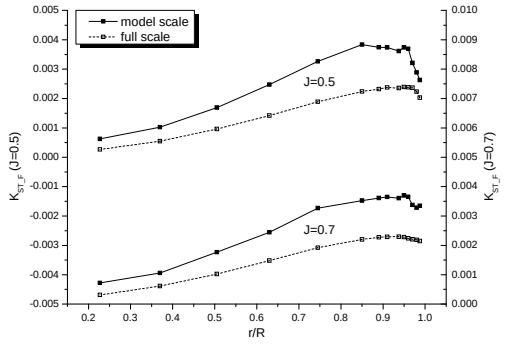

(b)

Figure 12 Comparison of the frictional component of section tangential forces for PPTC-II

A further discussion can be made on how the changes in section normal and tangential forces due to the scale effect influence those in propeller thrust and torque. As illustrated in Figure 13, the axial and circumferential force coefficients of a blade section are expressed as

$$\begin{cases} K_{SA} = K_{SN}\cos\phi - K_{ST}\sin\phi \\ K_{SC} = K_{SN}\sin\phi + K_{ST}\cos\phi \end{cases} \tag{3}$$

where ϕ is the geometric pitch angle of the blade section.

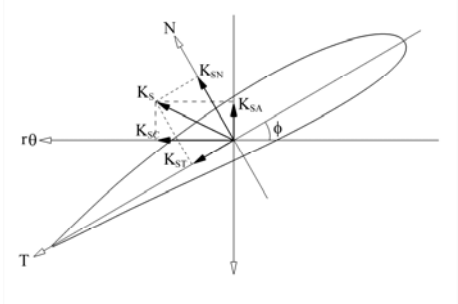

Figure 13 Relation of the axial and circumferential forces to the normal and tangential forces of a blade section

According to the results shown in Figures 7 through 12, the scale effects on K_{SN_F} and K_{ST_P} can be neglected. Then

$$\begin{cases} \Delta K_{SA} \approx \Delta K_{SN\_P}\cos\phi - \Delta K_{ST\_F}\sin\phi \\ \Delta K_{SC} \approx \Delta K_{SN\_P}\sin\phi + \Delta K_{ST\_F}\cos\phi \end{cases} \tag{4}$$

where Δ denotes the difference of full- and model-scale values. Since $\Delta K_{SN\_P} > 0$ and $\Delta K_{ST\_F} < 0$, it is clear that $\Delta K_{SA} > 0$; however, the sign of ΔK_{SC} depends on the magnitudes of ΔK_{SN_P} and ΔK_{ST_F}, as well as the pitch angle. But the contribution of ΔK_{SN_P} always cancel out that of ΔK_{ST_F} to some extent. Thus the analysis explains the reasons for the scale effects on propeller thrust and torque shown in Figure 5.

The present CFD results and analysis indicate that it might be necessary to take into account the scale effect on the thickness of blade surface boundary layer. Then the predicted scale effect can be equally important for both thrust and torque, or even primarily for the thrust.

3.3 Influence of Tip-Rake on Scale Effects

The PPTC-II is a propeller with the tip rake that is meant to load the tip (hence increase the efficiency) without creating strong tip vortices. It would be interesting to make a comparison of the scale effects on propellers with and without the tip rake. Therefore, the blade geometry of PPTC-II is modified by removing the tip rake, but keeping all the other geometric parameters untouched. The new propeller is named as PPTC-II-m, and the RANS simulations are carried out for it by using identical modeling approach and operating conditions to those for the PPTC-II. Figure 14 shows the geometric model of the PPTC-II-m.

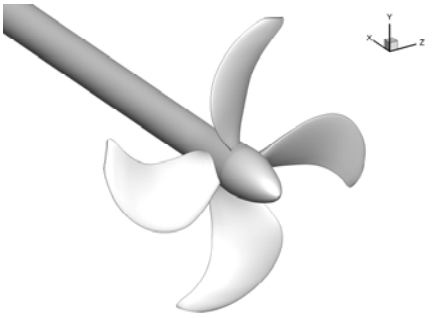

Figure 14 Geometric model of propeller PPTC-II-m

Figure 15 compares the open water performances yielded by RANS simulations for the PPTC-II-m at model- and full-scale, which are quite close to those for the PPTC-II except for extremely high/light loading conditions (J=0.1 and J=0.9).

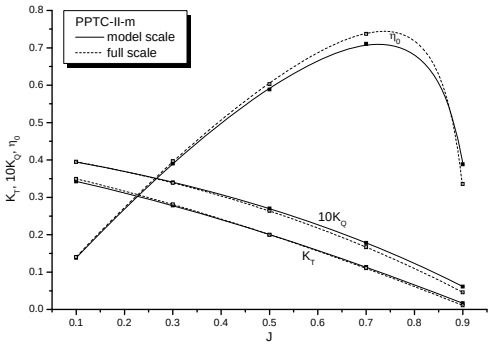

Figure 15 RANSE-predicted open water performances of PPTC-II-m at model- and full-scale

Figure 16 compares the scale effects on propeller thrust, torque, and efficiency for the PPTC-II and PPTC-II-m based on RANS simulation results. As seen in Figures 16(a) and 16(b), in light loading conditions (J=0.5 and

J=0.7), there are large differences between PPTC-II and PPTC-II-m in the scale effects on propeller thrust and torque. Figure 16(c) shows that the scale effect on propeller efficiency is generally larger for PPTC-II than for PPTC-II-m by 0.5%~1%.

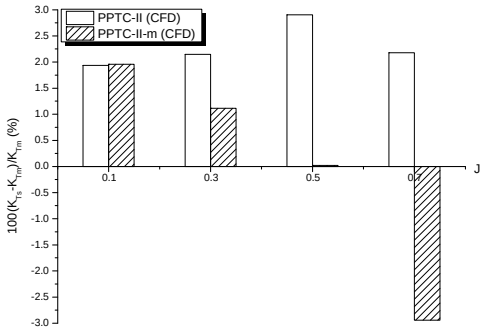

(a) thrust

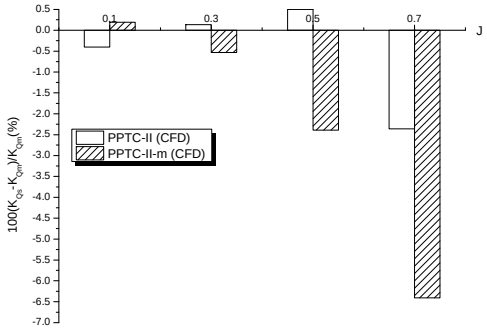

(b) torque

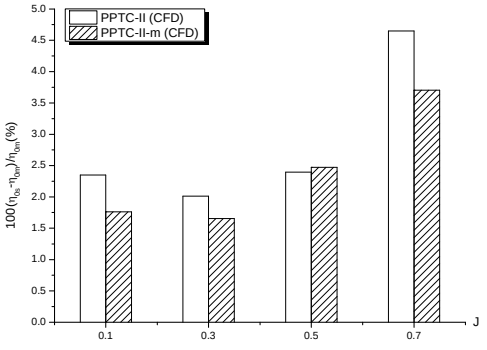

(c) efficiency

Figure 16 Comparison of RANS-predicted scale effects on the open water performances of PPTC-II and PPTC-II-m

Figures 17 and 18 show the results of sectional force analysis for propeller PPTC-II-m. By comparing Figures 17(a) and 17(b) it is obvious that the frictional force contributes little to the section normal force, which is the same as for the PPTC-II. However, as shown in Figure 17(b), ΔK_{SN_P} decreases from positive to negative value as J increases, which explains the results at J=0.5 and J=0.7 for PPTC-II-m in Figures 16(a) and 16(b).

Figures 18(a) and 18(b) indicate that, the frictional force is not the only contributor to the section tangential force, especially close to the tip. This is different from the results for PPTC-II (see Figures 10 and 11).

Besides, as shown in Figures 17 and 18, the monotonic increase in section normal force as well as the sharp increase in section tangential force close to the tip are both different from the case of PPTC-II. The tip rake actually reduces the loading close to the tip, especially when the angle of attack is small. By comparing Figures 19 and 20, the pressure fields in the cross sections immediately downstream of the tip trailing edge, it is clear that the tip vortices of PPTC-II are much weaker (due to reduced tip loading) than those of PPTC-II-m.

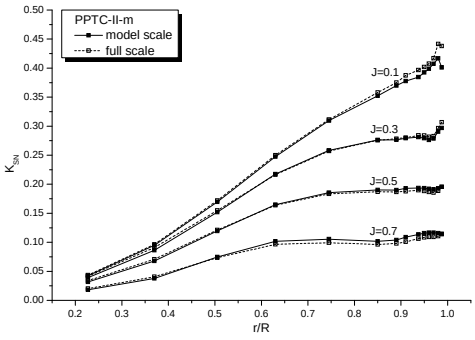

(a) total

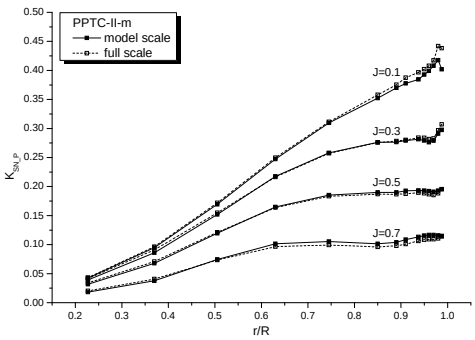

(b) pressure component

Figure 17 Section normal forces for PPTC-II-m

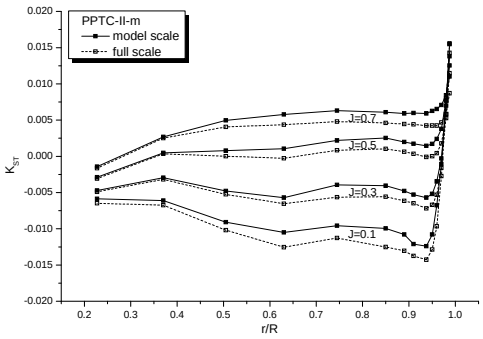

(a) total

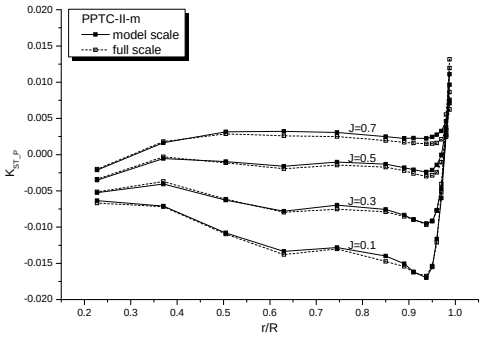

(b) pressure component

Figure 18 Section tangential forces for PPTC-II-m

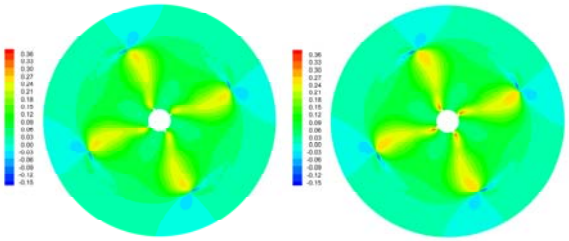

(a) model scale **(b) full scale**

Figure 19 RANS-simulated pressure fields in the cross section 0.005*D* downstream of the trailing edge of tip. PPTC-II, *J*=0.7.

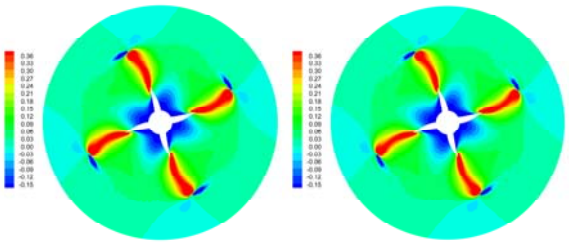

(a) model scale **(b) full scale**

Figure 20 RANS-simulated pressure fields in the cross section 0.005*D* downstream of the trailing edge of tip. PPTC-II-m, *J*=0.7.

Finally, the scale effects predicted by the ITTC method are compared with those by RANS simulations in Figure 21. Similar to the comparison made for the PPTC-II in Figure 6, the differences between ITTC and RANS results are large for K_T, but relatively small for K_Q. The ITTC-predicted increases in the full-scale efficiency of PPTC-II-m are still quite close to the RANS predictions, but are all higher than the latter.

4 CONCLUSIONS

Based on the RANS simulations, the scale effects on propeller open water performance have been numerically studied for PPTC-II, an ITTC benchmark propeller, and PPTC-II-m, a modified version of the PPTC-II by removing the tip rake. By analyzing the RANS-based blade section forces, and comparing the scale effects predicted by RANS with those by the ITTC-1978 method, the following conclusions are drawn,

1) The scale effect on propeller thrust can be as important as that on the torque, which seems to be the result of reduced boundary layer thickness on full-scale blade surfaces. On the contrary, the scale effect correction for K_T is one magnitude smaller than that for K_Q according to the ITTC method.

2) Although the corrections for K_T and K_Q by the ITTC method differ largely from those by the RANS method, the corrections for η_0 by the two methods agree quite well at least in the cases of PPTC-II and PPTC-II-m. Further investigations are necessary to find out if this is just a coincidence.

3) The tip rake serves to reduce the hydrodynamic loading close to the tip. At small angle of attack where the propeller is designed to work, large differences in the scale effects on K_T and K_Q are identified with and without the tip rake, but not on η_0. To account for the tip rake and predict the scale effects on K_T and K_Q more accurately, the existing ITTC method might need to be updated.

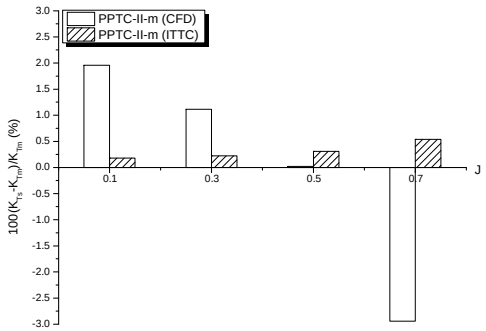

(a) thrust

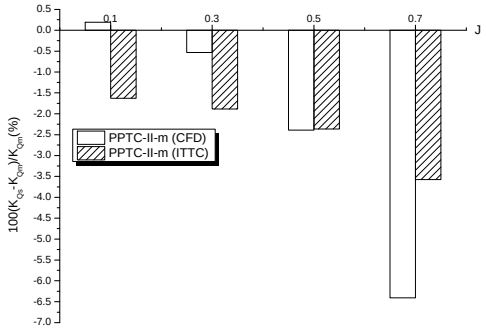

(b) torque

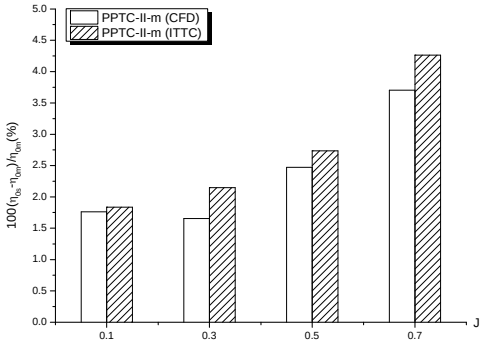

(c) efficiency

Figure 21 Comparison of RANS- and ITTC-predicted scale effects on the open water performance of PPTC-II-m

REFERENCES

Hsin, C.-Y., Chang, K.-K., Chi, R.-C. & Chen, P.-F. (2010). 'Design and Analysis of the End Plate Effect Propellers', Proceedings of the 28th Symposium on Naval Hydrodynamics, Pasadena, CA, USA.

International Towing Tank Conference (2014). '1978 ITTC Performance Prediction Method', ITTC - Recommended Procedures and Guidelines, 7.5-02-03-01.4, Revision 03.

Kawamura, T. & Omori, T. (2009). 'Reynolds Number Effect on Propeller Performance in Open Water', Journal of the Japan Society of Naval Architects and Ocean Engineers **10**, pp.29-36.

Krasilnikov, V. I., Sun, J. Y. & Halse, K. H. (2009). 'CFD Investigation in Scale Effect on Propellers with Different Magnitude of Skew in Turbulent Flow', Proceedings of the 1st International Symposium on Marine Propulsors, Trondheim, Norway.

Krasilnikov, V. I., Zhang, Z., Hong, F., Ponkratov, D. V. & Sun, J. Y. (2007). 'Steady Analysis of Viscous Flow around Ducted Propellers: Validation and Study on Scale Effects', Proceedings of the 9th International Conference on Fast Sea Transportation, Shanghai, China.

Müller, S. B, Abdel-Maksoud, M. & Hilbert, G. (2009). 'Scale Effects on Propellers for Large Container Vessels', Proceedings of the 1st International Symposium on Marine Propulsors, Trondheim, Norway.

Oh, S., Jang, J., Rhyu, S., Hoshino, T. & Seo, J. (2010). 'Some Applications on Extrapolation Method of Rudder Bulb Performance as an Energy-Saving Device', Proceedings of the 11th International Symposium on Practical Design of Ships and Other Floating Structures, Rio de Janeiro, Brazil.

Sánchez-Caja, A., González-Adalid, J., Pérez-Sobrino, M. & Sipilä, T. (2014). 'Scale Effects on Tip Loaded Propeller Performance Using a RANSE Solver', Ocean Engineering **88**, pp.607-617.

Stanier, M. (1998). 'The Application of RANS Code to Investigate Propeller Scale Effects', Proceedings of the 22nd Symposium on Naval Hydrodynamics, Washington DC, USA.

DISCUSSION

Question from Stephan Helma

What is the reason that the section force was split into components normal and tangential to the nose-tail pitch line and not normal and parallel to the hydrodynamic inflow?

Authors' closure

According to potential flow theory, the section lift is the only force perpendicular to the resultant inflow which is composed of the undisturbed inflow and the induced velocities. Inversely the resultant inflow direction can be found once the section force (without viscous component) is known. In viscous flow, however, it would be inappropriate to do so since the viscous force contributes (negatively) to the lift. In fact, we tried to determine the inflow direction by solving the Euler equations, but found erratic behaviors in section lift direction at inner radii (close to the hub), which was probably because the grid quality was not good enough in that region. For this reason, we eventually chose to use the nose-tail line for our analysis of the section forces.